Published in final edited form as:
Optom Vis Sci. 2014 May ; 91(5): 484–490. doi:10.1097/OPX.0000000000000249.

Between-Subject Variability in Asymmetry Analysis of Macular Thickness

Muhammed S. Alluwimi, MS, **William H. Swanson, PhD, FAAO**, and **Victor E. Malinovsky, OD. FAAO**
Indiana University School of Optometry, Bloomington, Indiana

Abstract

Purpose—To investigate the use of Asymmetry Analysis to reduce between-subject variability of macular thickness measurements using SD-OCT.

Methods—63 volunteers free of eye disease were recruited: 33 young subjects (ages 21 to 35 years), and 30 older subjects (ages 45 to 85 years). Macular images were gathered with the Spectralis OCT. An overlay 24°× 24° grid was divided into five zones per hemifield, and Asymmetry Analysis was computed as the difference between superior and inferior zone thicknesses. We hypothesized that the lowest variation and the highest density of ganglion cells will be found ~3° to 6° from the foveola, corresponding to zones 1 and 2. For each zone and age group, between-subject standard deviations (SDs) were compared for retinal thickness (RT) versus Asymmetry Analysis using an F-test. To account for repeated comparisons, a probability of $p < 0.0125$ was required for statistical significance. Axial length (AL) and corneal curvature (CC) were measured with an IOLMaster.

Results—For OD, Asymmetry Analysis reduced between-subject variability in zones 1 and 2 in both groups ($F > 3.2$, $p < 0.001$). SD for zone 1 dropped from 12.0 to 3.0μm in the young group and from 11.7 to 2.6μm in the older group. SD for zone 2 dropped from 13.6 to 5.3μm (young) and from 11.1 to 5.8μm (older). Combining all subjects, neither RT nor Asymmetry *Analysis* showed a strong correlation with AL or CC ($R^2 < 0.01$). Analysis for OS yielded the same pattern of results, as did Asymmetry Analyses between eyes ($F > 3.8$, $p < 0.0001$).

Conclusions—Asymmetry Analysis reduced between-subject variability in zones 1 and 2. Combining the five zones together produced a higher between-subject variation of the RT Asymmetry Analysis, thus we encourage clinicians to be cautious when interpreting the Asymmetry Analysis printouts.

Keywords

macular thickness; ganglion cells; Asymmetry Analysis; variability; glaucoma; OCT

Structural changes in patients with glaucoma have a crucial role in clinical diagnosis and management. Optical Coherence Tomography (OCT) has been widely used to image

Corresponding author: Muhammed S. Alluwimi, Indiana University School of Optometry, 800 East Atwater Ave, Bloomington, IN 47405, malluwim@indiana.edu.

The authors have no conflicts of interest.

structural features of glaucoma with a variety of imaging options. Retinal Nerve Fiber Layer (RNFL) thickness has been extensively investigated using OCT, but RNFL measurements have limitations that introduce substantial challenges in clinical decision-making. In this study we investigated a method intended to overcome some of these limitations using macular thickness measurements.

RNFL thickness has high between-individual variability[1–3] and can be affected by magnification factors such as axial length[4–6] and corneal curvature.[7] Optic disc and rim area measurements also exhibit high between-subject variability among control subjects.[8–10] Moreover, blood vessels can contribute to measured average RNFL thickness,[11] as can glial cells,[12] with substantial variability among individuals. In histological studies of human eyes, between-subject variability in the total number of ganglion cells and their axons showed a two-fold range.[13–15] The lowest between-subject variability in ganglion cell density was observed within 0.5 to 1 mm eccentricity from the foveal center[13, 14] which may be related to active control processes during embryological development. The number of ganglion cells is substantially reduced during development, and is a source of variability among individuals.[16, 17]

Recently, OCT has been used to measure retinal thickness of the macula in patients with glaucoma.[18–22] Although OCT can provide precise retinal thickness measurements, there are limitations such as the low reflectivity of the ganglion cell layer. Moreover, differences in magnification factors such as axial length and refractive error among individuals can influence the accuracy of retinal thickness measurements.[18, 23–25] These factors can contribute to between-subject variability. It has been estimated that around 50% of ganglion cells are found within ±8.0° eccentricity from the foveola,[13] therefore, between-subject variation in ganglion cell density in this region may be an important factor in analysis of macular thickness. Posterior Pole Asymmetry Analysis has been recently introduced with Spectralis OCT (Heidelberg Engineering, V 5.4, Heidelberg, Germany), to compare macular thickness within and between eyes of an individual.[26] The within-eye Asymmetry Analysis calculates the difference in retinal thickness between superior and inferior cells in 64-cell square grid superimposed on a 24°×24° retinal region centered on the foveola. In this new protocol, a gray scale has been used to indicate asymmetries in retinal thickness within and between eyes. On this scale, white is used to represent no asymmetry in retinal thickness, light gray to dark gray represent asymmetries from approximately 5 to 25 microns, and black represents greater asymmetries of more than 25 microns. However, black cells in the Asymmetry Analysis may not be uncommon in subjects free of eye disease.[27] Therefore more investigation is warranted to better understand the gray scale for the Asymmetry Analysis grid. In this study, we assessed Asymmetry Analysis as a method for reducing between-subject variability.

METHODS

Participants

Two groups of volunteers free of eye disease were recruited: thirty-three young subjects were recruited from students at the Indiana University School of Optometry (ages 21 to 35 with mean and SD of 25.0 ± 1.7 years). Thirty older subjects were recruited from control

subjects in an ongoing study of patients with glaucoma (ages 45 to 85 with mean and SD of 66.7 ± 9.0 years) at the optometry clinic of Indiana University Bloomington. All subjects were considered free of eye disease after a comprehensive ophthalmic examination: normal visual field, IOP < 21mm Hg, normal optic cup-disc ratio, open anterior chamber angles and best corrected visual acuity of 20/20 or better. Subjects with a history of ocular disease or eye surgery were excluded except those who had uncomplicated cataract surgery more than six months prior to testing.

Equipment

Macular images were gathered with the Spectralis OCT, using the Posterior Pole Protocol from the Pretest for the Glaucoma Application. For both groups, macular images of both eyes were acquired by one of the authors (MA). Axial length and corneal curvature were measured using an IOLMaster (Carl Zeiss Meditec, V. 5.02, Jena, Germany) by the same operator during the same session. In order to ensure accurate corneal curvature measurements, subjects who wore contact lenses were instructed to remove their lenses at least 12 hours before their appointment. The study goals and procedures were explained to the participants, and informed consent was obtained from each participant prior to testing. This study followed the tenets of Declaration of Helsinki and was approved by the Indiana University institutional review board (IRB).

Spectralis OCT

The Posterior pole protocol was applied to image both eyes in all subjects, providing 61 B-scans 120 microns apart for each scan, with optical resolution of 7 μm axially and 14 μm laterally. Subjects were asked to fixate on an internal blue fixation target in the Spectralis camera. The camera was centered on the fovea with even illumination within a 6×6 mm area. For some subjects the fellow eye was occluded to help maintain fixation. Lubricating eye drops were used as needed. The OCT image quality score was required to be 25 or greater, any image with score below that limit was excluded. Dr. Malinovsky, a specialist in ocular disease, reviewed each B-scan to determine that there was no evidence of retinal abnormality. Two subjects in the older group were excluded due to poor image quality.

As shown in Figure 1, the retinal thickness grid overlays a 24°× 24° retinal region centered on the measured area of 30°× 25°. This grid is composed of 64 cells; each cell represents the average measured retinal thickness of a 3°×3° area. The operator realigned and centered the grid on the fovea when needed, and rotated the central line of the grid to align with the foveal-optic disc axis. The Spectralis performs automated segmentation from the Inner Limiting Membrane (ILM) to the Bruch's Membrane (BM). For two subjects the automated segmentation failed for six B-scans, which were re-segmented manually by the operator.

Analysis

For the primary analysis, our goal was to determine whether within-eye Asymmetry Analysis reduced between-subject variability for averages across cells in five zones per hemifield, using the approach developed by Um et al,[28] as shown in Figure 1. The within-eye Asymmetry was computed as the difference between retinal thicknesses of superior and inferior grids (superior minus inferior, so that a negative number means that the inferior cell

had greater thickness). The computation was only for subtracting the inferior from corresponding superior locations of retinal thicknesses (S I) to avoid zero values when averaging the superior and inferior asymmetries of the grid. We hypothesized that the lowest variability would be in the region 0.5 to 1 mm from the foveola,[13, 14] because the histological data of Curcio and Allen[13] had the lowest between-subject variability in this region, and the greatest superior/inferior symmetry. In order to maintain sufficient statistical power, we focused on zones 1 and 2 (approximately 3° to 6° from the central line of the grid) for evaluating the ability of the within-eye Asymmetry Analysis to reduce between-subject variability. For each age group and zone, an F-test was used to compare the variance for the averaged superior and inferior retinal thicknesses with the variance for the within-eye Asymmetry Analyses. A significance level of $p < 0.0125$ was required for interpretation as statistically significant, after Bonferroni correction for use of 4 tests. For descriptive statistics, bivariate Gaussian ellipses were plotted[29] to indicate 95% of the distribution for within-eye Asymmetry Analyses versus retinal thicknesses in zones 1 and 2 as compared with the sum across all five zones. To allow comparisons with other studies, Analysis of Variance (ANOVA) was used to evaluate the effect of age group on the retinal thickness measurements and the within the eye Asymmetry Analysis (right eye).

In the secondary analysis, we evaluated a gray scale that we created for retinal thickness as difference from mean normal, and the gray scale for within-eye Asymmetry Analysis with the intent to gain a better understanding of the clinical usefulness of printouts provided by the Spectralis OCT. For each cell we, computed the 5th percentile as 1.64 SDs for one-tailed limits (retinal thickness grid), because clinical decision-making identifies defects by asking whether thickness is below mean normal. We computed the 2.5th percentile as 1.96 SDs for two-tailed limits (within-eye Asymmetry Analysis grid from our data results) because either direction can indicate a defect.

In order to compare our data with histological data, we estimated the ganglion cell contribution to the retinal thickness by analyzing data from patients with non-seeing locations in their macular visual fields. We then subtracted the lowest measured retinal thicknesses from the mean measured retinal thickness of our subjects free of eye disease in the corresponding cell and hemifield, and estimated that the ganglion cells represent approximately 25% of the retinal thickness within 3° to 6° from the foveola. This estimate is consistent with estimates of the ganglion cell layer thickness in histological studies[30] and in OCT studies with manual segmentation.[31, 32]

RESULTS

Across the 14 individual cells of zones 1 and 2, SDs for retinal thickness measurements ranged from 11.4 μm to 14.9 μm with a mean of 13.5 μm in the young group, and from 9.6 to 15.8 μm with a mean of 12.6 μm in the older group. Means and SDs for retinal thickness were 331.5 ± 12.0 μm in zone 1 and 333.0 ± 13.7 μm in zone 2 in the young group. In the older group, means and SDs were 326.6 ± 11.7 μm in zone 1 and 320.7 ± 11.1 μm in zone 2. Within-eye Asymmetry Analysis significantly reduced the between-subject variability in zones 1 and 2 in both groups ($F > 3.2$, $p < 0.001$). In the young group, SD declined from

12.0 to 3.0 μm in zone 1, and from 13.7 to 5.3 μm in zone 2. In the older group, SD declined from 11.7 to 2.6 μm in zone 1 and from 11.1 to 5.8 μm in zone 2.

Figure 2 shows data for within-eye Asymmetry Analysis results versus retinal thickness along with ellipses that represent 95% of between-subject variability based on SDs. The left panel shows data when all five zones were combined: for both groups the between-subject variability was higher for Asymmetry Analysis than for retinal thickness. The right panel shows data for zones 1 and 2 combined: for both groups the between-subject variability in the retinal thickness was similar to the left panel, while between-subject variability in within-eye Asymmetry Analysis results was substantially reduced.

The between-eye Asymmetry Analysis for zones 1 and 2 also showed a significant reduction in variability ($F > 3.8$, $p < 0.0001$). The highest between-subject variability was found in zone 5 for both groups; means and SDs were 301.5±15.4 μm in the young group and 293.1±14.6 μm in the older group. For both groups, means, SDs and coefficients of variation (CoVs) for all five zones are given in Table 1. Retinal thickness was significantly reduced in the older group ($F = 16.01$, $p < 0.0001$). However, within-eye Asymmetry Analysis did not show a significant difference between the young and older groups ($F = 2.36$, $p = 0.13$).

Figure 3 shows the retinal thickness and within-eye Asymmetry Analysis grids from right eyes of the young group. We found that the normal range in the current study included values shown as gray to black in the Asymmetry Analysis printout (Figure 3, right panel). The greatest reduction in variability from retinal thickness to Asymmetry Analysis grids was in zones 1 and 2, on which we focused for hypothesis-testing. The locations with the highest between-subject variability reflect blood vessel patterns in both grids. Similar results were also found for the older subjects in our analysis.

Based on our estimate of the ganglion cell contribution to retinal thickness, within-eye Asymmetry Analysis showed a significant reduction in the between-subject variability of the ganglion cell component. For the estimated ganglion cell contribution to zone 1 thickness, SD was reduced from 0.15 to 0.04 μm in young group and from 0.14 to 0.03 μm in the older group. This reduction was also observed in the estimated ganglion cell contribution in zone 2; SD declined from 0.17 to 0.06 μm in the young group, and from 0.14 to 0.07 μm in the older group ($F > 3.1$, $p < 0.001$). Axial length and corneal curvature did not show a strong correlation with either retinal thickness or Asymmetry Analysis ($R^2 < 0.01$). For the younger group, means and SDs were 24.59 ± 0.95 mm for axial length and 7.77 ± 0.29 mm for corneal curvature. The means and SDs for the older subjects were 24.03 ± 1.08 mm for axial length in and 7.70 ± 0.30 mm for corneal curvature.

DISCUSSION

In this study we focused on zones 1 and 2 of Um et al,[28] which as shown in Figure 1 include retinal thicknesses from 3° to 6° from the center of the fovea. This region has been reported to have the highest density and the lowest between-subject variability of retinal ganglion cells.[13] Averaging the retinal thickness using these zones did not reduce between-subject variability below that for individual cells. By comparison, the difference in retinal thickness

between corresponding locations in the superior and inferior hemifields (within-eye Asymmetry Analysis) successfully reduced between-subject variability in zones 1 and 2 as compared to Asymmetry Analyses for all five zones added together (figure 2). Results of Asymmetry Analysis in our study (shown in table 1) were similar to those in Um et al for all five zones except zone 1.

In figure 3, it can be observed that between-subject variability decreased in zones 1 and 2 in the within-eye asymmetry grid, while in other zones variability was still high and flagged as dark gray to black. This implies that the current gray scale for the asymmetry grid could present a misleading impression of macular damage in eyes free of disease. Therefore, we encourage clinicians to be cautious when interpreting the Asymmetry Analysis grid. Seo et al.[27] reported that about 19% of their subjects free of disease had two or more consecutive black cells in the asymmetry grid. For instance, blood vessels are included in the superior and inferior arcades, which may cause consecutive black cells to be seen in healthy control subjects.

Zeimer, Asrani and colleagues were the first to measure human retinal thickness with laser technology.[33, 34] They focused on a 2×2 mm^2 area of the posterior pole excluding the foveola, which is similar to the area that we included in our study. In their analysis, they calculated the deviation from the normal retinal thicknesses for each hemifield, and then differences in that deviation between the superior and inferior hemifields. In a control study, Asrani et al.[34] reported that the SD of the retinal thickness was ±15 μm for 29 normal subjects aged from 19 to 76, which is similar to ours (±12 μm); age did not show a significant effect on the measured retinal thickness in their data. The design of the current study included two age groups, and retinal thickness was found to be significantly reduced in the older group.

In 20 normal subjects and 20 patients with glaucoma, Bagga et al.[22] found a low CoV (3.81%) for the retinal thickness of their control subjects using Stratus OCT, which is similar to what we found in our study (3.57%). They applied two radial scans and focused on 8° temporal to the fovea. In the current study we focused on both 6° temporal and 6° nasal to the fovea. In addition, the mean and SDs of the Asymmetry Analysis of our data were extended to two different locations (zones 1 and 2) in each hemifield with separate groups of young and older subjects.

Zeimer and colleagues[33] estimated that ganglion cells may represent 30 to 35% of the retinal thickness in the posterior pole. Spectralis OCT measures the entire thickness of the retina, but does not measure the ganglion cell layer thickness. Previous studies attempted to segment out both the Retinal Ganglion Cell layer and the Inner Plexiform Layer (GCL + IPL) using other SD-OCTs either by manual segmentation[31, 32] or automated segmentation.[35, 36] SDs for these studies (5.1 μm for Wang et al.; 6.2 μm for Mwanza; and 7.0 μm for Koh) were lower than those we found for the retinal thickness in zones 1 and 2 (11.9 μm and 13.6 μm respectively) in both groups. This difference may be due to more non-ganglion cell components in retinal thickness than in segmented GCL. It is important to note that the Spectralis automated segmentation spans the region from the ILM to Bruch's membrane. Thus, Henle fibers can contribute some of the between subject-variability. It has

been found that Henle fibers have their highest variability within 0.3 to 1.2 mm eccentricity from the foveola.[30] GCL segmentation, on the other hand, is extended beyond ±6° (zones 1 and 2) and includes the IPL layer. Knighton et al.[37] also used manual segmentation of GCL +ILP in SD-OCT, and suggested that the variance of the normal population (23 subjects) could be decreased by transforming the reference normal GCL+ILP thickness maps to a standard form, better allowing abnormal GCL+ILP thickness maps to be distinguished.

We estimated that ganglion cell components compose 25% of normal reference means for retinal thickness in zones 1 and 2 in our sample, which is consistent with other previous studies using histology[30] and imaging techniques.[31–33] Within-eye Asymmetry Analysis was still able to reduce between-subject variability of our estimates of ganglion cell components in these zones.

However, our estimate of the ganglion cell component should be investigated more closely since there are sources of variability that can cause an inaccurate estimation of the ganglion cell components of retinal thickness measured with the Spectralis OCT. Retinal thickness reduced significantly with age in the current study, and this reduction is in agreement with the previously reported reduction in ganglion cells in histological studies.[14, 30, 38] An age-related reduction in retinal thickness was also reported in other imaging studies.[39, 40] It has been suggested that non-neural components of the RNFL increase with age in response to the death of ganglion cells.[41] Therefore, age is a factor that should be considered when estimating the ganglion cell component of the retinal thickness. Our results showed that asymmetry of retinal thickness did not differ significantly between the young and older groups. This indicates the potential of within-eye Asymmetry Analysis of the retinal thickness in zones 1 and 2 to successfully reduce between-subject variability due to age.

By choosing zones 1 and 2 in particular, we also tried to reduce the effect of the blood vessels on retinal thickness, which is another source of between-subject variability.[11] However, there were still some small blood vessels in these two zones. Blood vessels may also have variable patterns and sizes among individuals that make them have a notable effect on between-subject variability in retinal thickness. Segmenting out the blood vessels, as has already been done in the retinal nerve fiber layer (RNFL) in some studies,[42] may decrease between-subject variability. In the GCL+ILP manual segmentation using SD-OCT where blood vessels were removed,[32] a lower SD was reported (5.1 μm) than what we found in our studies (11.9 μm in zone 1 and 13.6 μm in zone 2). Therefore, it may be worthwhile to apply these segmentation methods to the retinal thickness in order to look at the zones that have larger blood vessels than zones 1 and 2.

Ganglion cells represent a small proportion of macular thickness: this proportion has high between-subject variability that can lead to difficulties in diagnosing ganglion cell loss. One approach is to estimate GCL thickness by segmenting out GCL + IPL. However, Raza[31] estimated that non-ganglion cell components comprise approximately 50% of the initial control median RGC + IPL thickness at 3.4° from the foveola, and 80% of the initial control median RGC + IPL thickness at 8.8°from the foveola. The within-eye Asymmetry Analysis results in the current study showed a potential reduction in between-subject variability of the macular thickness. Our data showed that within-individual variability of retinal thickness

measurements is relatively small in comparison to between-subject variability. These results are consistent with histological findings of Curcio and Allen[13] and with findings of other OCT studies.[43, 44] Asymmetry Analysis should be helpful in reducing the impact of the non-ganglion cell components, particularly in our zones 1 and 2.

Within-eye Asymmetry Analysis reduced between-subject variability in our study, indicating a potential diagnostic technique for glaucomatous damage. Further investigation is needed to confirm the capability of the within-eye Asymmetry Analysis in reducing between-subject variability, including a larger sample of subjects free of eye disease. Sources of variability such as age, blood vessels and magnification factors should be considered when obtaining retinal thickness measurements. By using the zones of Um et al,[28] retinal thicknesses in the superior and inferior zones 1 and 2 were found to be almost identical. This result might be helpful in detecting defects in macular ganglion cells, which have been reported to most likely occur as an asymmetric defect.[45] It would be valuable to compare within-eye Asymmetry Analysis of macular thickness to visual field loss, which may lead to a better understanding of the structure-function relations.

Acknowledgments

This study was supported by NIH grant R01EY007716 (WHS).

References

1. Hood DC, Salant JA, Arthur SN, Ritch R, Liebmann JM. The location of the inferior and superior temporal blood vessels and interindividual variability of the retinal nerve fiber layer thickness. J Glaucoma. 2010; 19:158–66. [PubMed: 19661824]
2. Hong SW, Ahn MD, Kang SH, Im SK. Analysis of peripapillary retinal nerve fiber distribution in normal young adults. Invest Ophthalmol Vis Sci. 2010; 51:3515–23. [PubMed: 20164448]
3. Tariq YM, Li H, Burlutsky G, Mitchell P. Retinal nerve fiber layer and optic disc measurements by spectral domain OCT: normative values and associations in young adults. Eye (Lond). 2012; 26:1563–70. [PubMed: 23079750]
4. Savini G, Barboni P, Parisi V, Carbonelli M. The influence of axial length on retinal nerve fibre layer thickness and optic-disc size measurements by spectral-domain OCT. Br J Ophthalmol. 2012; 96:57–61. [PubMed: 21349942]
5. Kang SH, Hong SW, Im SK, Lee SH, Ahn MD. Effect of myopia on the thickness of the retinal nerve fiber layer measured by Cirrus HD optical coherence tomography. Invest Ophthalmol Vis Sci. 2010; 51:4075–83. [PubMed: 20237247]
6. Yoo YC, Lee CM, Park JH. Changes in peripapillary retinal nerve fiber layer distribution by axial length. Optom Vis Sci. 2012; 89:4–11. [PubMed: 21983121]
7. Patel NB, Garcia B, Harwerth RS. Influence of anterior segment power on the scan path and RNFL thickness using SD-OCT. Invest Ophthalmol Vis Sci. 2012; 53:5788–98. [PubMed: 22836769]
8. Medeiros FA, Zangwill LM, Bowd C, Weinreb RN. Comparison of the GDx VCC scanning laser polarimeter, HRT II confocal scanning laser ophthalmoscope, and stratus OCT optical coherence tomograph for the detection of glaucoma. Arch Ophthalmol. 2004; 122:827–37. [PubMed: 15197057]
9. Bowd C, Zangwill LM, Medeiros FA, Tavares IM, Hoffmann EM, Bourne RR, Sample PA, Weinreb RN. Structure-function relationships using confocal scanning laser ophthalmoscopy, optical coherence tomography, and scanning laser polarimetry. Invest Ophthalmol Vis Sci. 2006; 47:2889–95. [PubMed: 16799030]

10. Leung CK, Cheung CY, Lin D, Pang CP, Lam DS, Weinreb RN. Longitudinal variability of optic disc and retinal nerve fiber layer measurements. Invest Ophthalmol Vis Sci. 2008; 49:4886–92. [PubMed: 18539940]
11. Hood DC, Fortune B, Arthur SN, Xing D, Salant JA, Ritch R, Liebmann JM. Blood vessel contributions to retinal nerve fiber layer thickness profiles measured with optical coherence tomography. J Glaucoma. 2008; 17:519–28. [PubMed: 18854727]
12. Ogden TE. Nerve fiber layer of the primate retina: thickness and glial content. Vision Res. 1983; 23:581–7. [PubMed: 6612997]
13. Curcio CA, Allen KA. Topography of ganglion cells in human retina. J Comp Neurol. 1990; 300:5–25. [PubMed: 2229487]
14. Blanks JC, Torigoe Y, Hinton DR, Blanks RH. Retinal pathology in Alzheimer's disease. I. Ganglion cell loss in foveal/parafoveal retina. Neurobiol Aging. 1996; 17:377–84. [PubMed: 8725899]
15. Jonas JB, Schmidt AM, Muller-Bergh JA, Schlotzer-Schrehardt UM, Naumann GO. Human optic nerve fiber count and optic disc size. Invest Ophthalmol Vis Sci. 1992; 33:2012–8. [PubMed: 1582806]
16. Rakic P, Riley KP. Overproduction and elimination of retinal axons in the fetal rhesus monkey. Science. 1983; 219:1441–4. [PubMed: 6828871]
17. Provis JM, van Driel D, Billson FA, Russell P. Human fetal optic nerve: overproduction and elimination of retinal axons during development. J Comp Neurol. 1985; 238:92–100. [PubMed: 4044906]
18. Leung CK, Cheung CY, Weinreb RN, Lee G, Lin D, Pang CP, Lam DS. Comparison of macular thickness measurements between time domain and spectral domain optical coherence tomography. Invest Ophthalmol Vis Sci. 2008; 49:4893–7. [PubMed: 18450592]
19. Greenfield DS, Bagga H, Knighton RW. Macular thickness changes in glaucomatous optic neuropathy detected using optical coherence tomography. Arch Ophthalmol. 2003; 121:41–6. [PubMed: 12523883]
20. Guedes V, Schuman JS, Hertzmark E, Wollstein G, Correnti A, Mancini R, Lederer D, Voskanian S, Velazquez L, Pakter HM, Pedut-Kloizman T, Fujimoto JG, Mattox C. Optical coherence tomography measurement of macular and nerve fiber layer thickness in normal and glaucomatous human eyes. Ophthalmology. 2003; 110:177–89. [PubMed: 12511364]
21. Jaffe GJ, Caprioli J. Optical coherence tomography to detect and manage retinal disease and glaucoma. Am J Ophthalmol. 2004; 137:156–69. [PubMed: 14700659]
22. Bagga H, Greenfield DS, Knighton RW. Macular symmetry testing for glaucoma detection. J Glaucoma. 2005; 14:358–63. [PubMed: 16148583]
23. Wu PC, Chen YJ, Chen CH, Chen YH, Shin SJ, Yang HJ, Kuo HK. Assessment of macular retinal thickness and volume in normal eyes and highly myopic eyes with third-generation optical coherence tomography. Eye (Lond). 2008; 22:551–5. [PubMed: 17464309]
24. Lam DS, Leung KS, Mohamed S, Chan WM, Palanivelu MS, Cheung CY, Li EY, Lai RY, Leung CK. Regional variations in the relationship between macular thickness measurements and myopia. Invest Ophthalmol Vis Sci. 2007; 48:376–82. [PubMed: 17197557]
25. Harb E, Hyman L, Fazzari M, Gwiazda J, Marsh-Tootle W. Factors associated with macular thickness in the COMET myopic cohort. Optom Vis Sci. 2012; 89:620–31. [PubMed: 22525127]
26. Asrani S, Rosdahl JA, Allingham RR. Novel software strategy for glaucoma diagnosis: asymmetry analysis of retinal thickness. Arch Ophthalmol. 2011; 129:1205–11. [PubMed: 21911669]
27. Seo JH, Kim TW, Weinreb RN, Park KH, Kim SH, Kim DM. Detection of localized retinal nerve fiber layer defects with posterior pole asymmetry analysis of spectral domain optical coherence tomography. Invest Ophthalmol Vis Sci. 2012; 53:4347–53. [PubMed: 22577076]
28. Um TW, Sung KR, Wollstein G, Yun SC, Na JH, Schuman JS. Asymmetry in hemifield macular thickness as an early indicator of glaucomatous change. Invest Ophthalmol Vis Sci. 2012; 53:1139–44. [PubMed: 22247461]
29. Altman DG. Plotting probability ellipses. J Roy Stat Soc Ser C (Appl Stat). 1978; 27:347–9.

30. Curcio CA, Messinger JD, Sloan KR, Mitra A, McGwin G, Spaide RF. Human chorioretinal layer thicknesses measured in macula-wide, high-resolution histologic sections. Invest Ophthalmol Vis Sci. 2011 Jun 6; 52(7):3943–54.10.1167/iovs.10-6377 [PubMed: 21421869]

31. Raza AS, Cho J, de Moraes CG, Wang M, Zhang X, Kardon RH, Liebmann JM, Ritch R, Hood DC. Retinal ganglion cell layer thickness and local visual field sensitivity in glaucoma. Arch Ophthalmol. 2011; 129:1529–36. [PubMed: 22159673]

32. Wang M, Hood DC, Cho JS, Ghadiali Q, De Moraes GV, Zhang X, Ritch R, Liebmann JM. Measurement of local retinal ganglion cell layer thickness in patients with glaucoma using frequency-domain optical coherence tomography. Arch Ophthalmol. 2009; 127:875–81. [PubMed: 19597108]

33. Zeimer R, Asrani S, Zou S, Quigley H, Jampel H. Quantitative detection of glaucomatous damage at the posterior pole by retinal thickness mapping. A pilot study Ophthalmology. 1998; 105:224–31.

34. Asrani S, Zou S, d'Anna S, Vitale S, Zeimer R. Noninvasive mapping of the normal retinal thickness at the posterior pole. Ophthalmology. 1999; 106:269–73. [PubMed: 9951475]

35. Mwanza JC, Durbin MK, Budenz DL, Girkin CA, Leung CK, Liebmann JM, Peace JH, Werner JS, Wollstein G. Profile and predictors of normal ganglion cell-inner plexiform layer thickness measured with frequency-domain optical coherence tomography. Invest Ophthalmol Vis Sci. 2011; 52:7872–9. [PubMed: 21873658]

36. Koh VT, Tham YC, Cheung CY, Wong WL, Baskaran M, Saw SM, Wong TY, Aung T. Determinants of ganglion cell-inner plexiform layer thickness measured by high-definition optical coherence tomography. Invest Ophthalmol Vis Sci. 2012; 53:5853–9. [PubMed: 22836772]

37. Knighton RW, Gregori G, Budenz DL. Variance reduction in a dataset of normal macular ganglion cell plus inner plexiform layer thickness maps with application to glaucoma diagnosis. Invest Ophthalmol Vis Sci. 2012; 53:3653–61. [PubMed: 22562512]

38. Kerrigan-Baumrind LA, Quigley HA, Pease ME, Kerrigan DF, Mitchell RS. Number of ganglion cells in glaucoma eyes compared with threshold visual field tests in the same persons. Invest Ophthalmol Vis Sci. 2000; 41:741–8. [PubMed: 10711689]

39. Ooto S, Hangai M, Tomidokoro A, Saito H, Araie M, Otani T, Kishi S, Matsushita K, Maeda N, Shirakashi M, Abe H, Ohkubo S, Sugiyama K, Iwase A, Yoshimura N. Effects of age, sex, and axial length on the three-dimensional profile of normal macular layer structures. Invest Ophthalmol Vis Sci. 2011; 52:8769–79. [PubMed: 21989721]

40. Song WK, Lee SC, Lee ES, Kim CY, Kim SS. Macular thickness variations with sex, age, and axial length in healthy subjects: a spectral domain-optical coherence tomography study. Invest Ophthalmol Vis Sci. 2010; 51:3913–8. [PubMed: 20357206]

41. Harwerth RS, Wheat JL, Rangaswamy NV. Age-related losses of retinal ganglion cells and axons. Invest Ophthalmol Vis Sci. 2008; 49:4437–43. [PubMed: 18539947]

42. Patel NB, Luo X, Wheat JL, Harwerth RS. Retinal nerve fiber layer assessment: area versus thickness measurements from elliptical scans centered on the optic nerve. Invest Ophthalmol Vis Sci. 2011; 52:2477–89. [PubMed: 21220552]

43. El-Ashry M, Hegde V, James P, Pagliarini S. Analysis of macular thickness in British population using optical coherence tomography (OCT): an emphasis on interocular symmetry. Curr Eye Res. 2008; 33:693–9. [PubMed: 18696345]

44. Wagner-Schuman M, Dubis AM, Nordgren RN, Lei Y, Odell D, Chiao H, Weh E, Fischer W, Sulai Y, Dubra A, Carroll J. Race- and sex-related differences in retinal thickness and foveal pit morphology. Invest Ophthalmol Vis Sci. 2011; 52:625–34. [PubMed: 20861480]

45. Raza AS, Zhang X, De Moraes CG, Reisman C, Liebmann JM, Ritch R, Hood DC. Improving glaucoma detection using spatially correspondent clusters of damage and by combining standard automated perimetry and optical coherence tomography. Invest Ophthalmol Vis Sci. 2014; 55:612–24. [PubMed: 24408977]

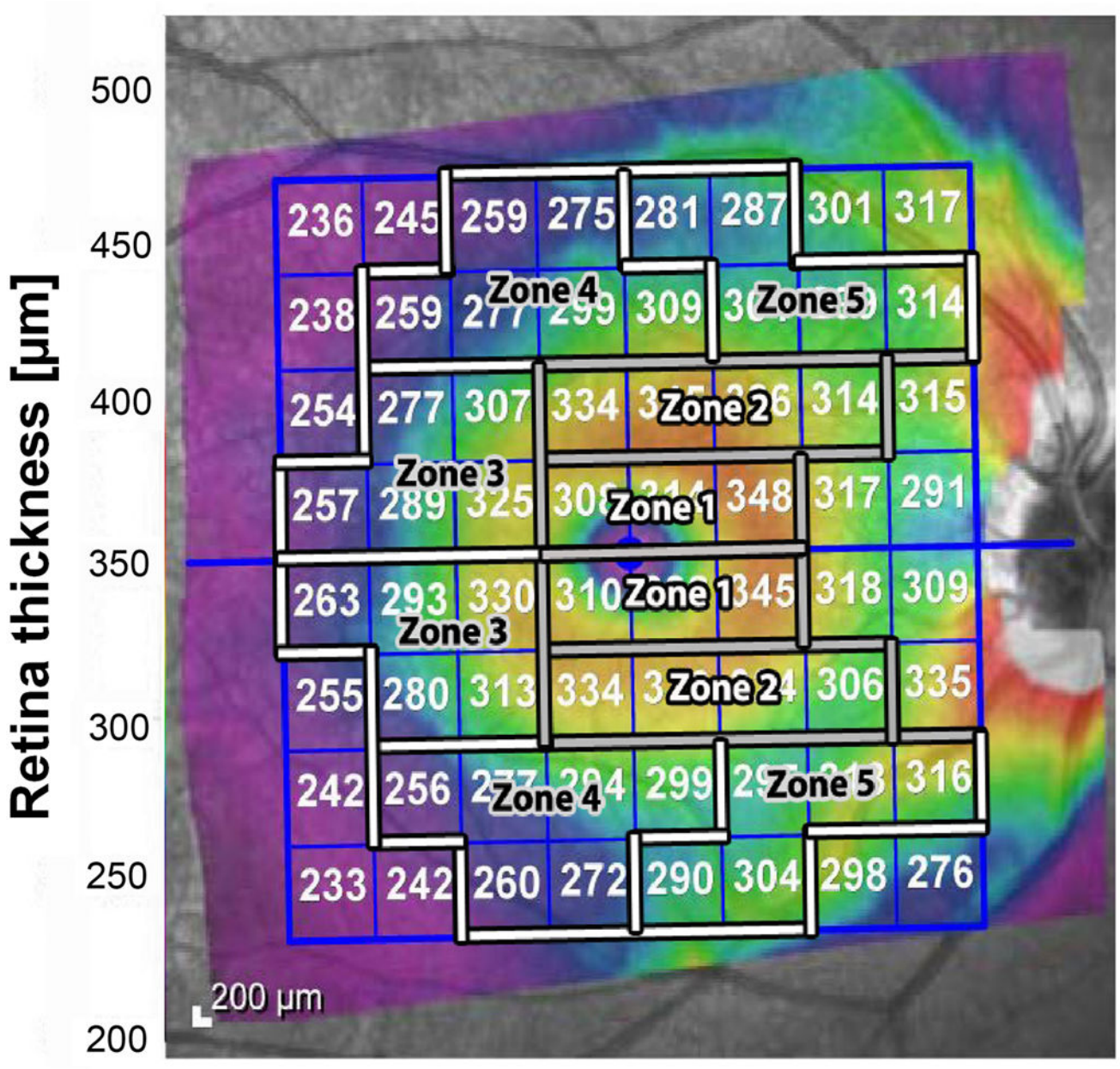

Figure 1.

Spectralis printout (right eye) showing the measurements of the average retinal thickness in each cell of the posterior pole grid. We drew lines that demarcate the five zones using the method of Um et al.[28] Superior and inferior hemifields of zones 1 and 2 are outlined by the gray rectangles with black edges. A color version of this figure is available online at www.optvissci.com.

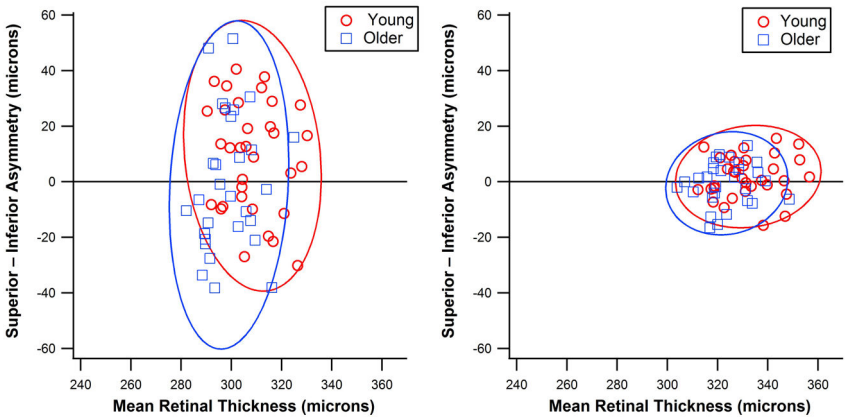

Figure 2.

Asymmetry Analyses between superior and inferior retinal thicknesses as a function of the averaged retinal thicknesses for the two age groups (young and older). Circles (young) and triangles (older) represent values for individual subjects; Ellipses represent 95% of the normal distribution. The left panel shows results when all five zones were combined and the right panel shows a substantial reduction in between subject variability when only zones 1 and 2 were combined. A color version of this figure is available online at www.optvissci.com.

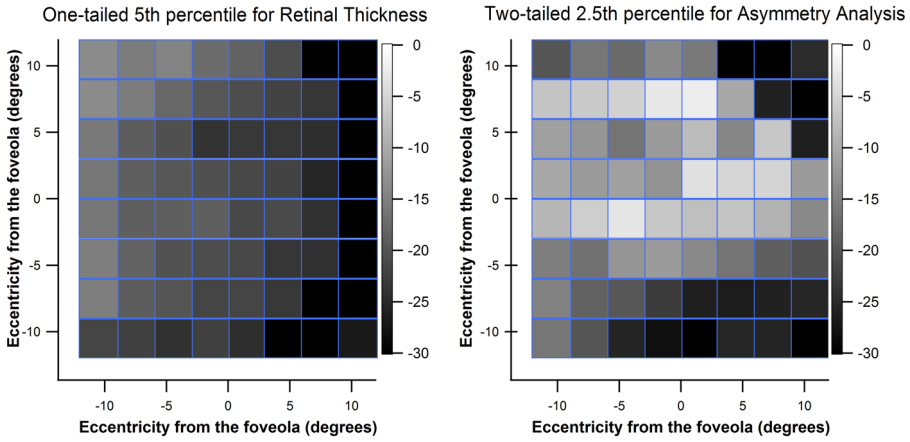

Figure 3.

Gray scale grids for the right eyes of young subjects free of eye disease. Left panel is for the one-tailed 5th percentile for our retinal thickness grid. Right panel shows the two-tailed 2.5th percentile for the within-eye Asymmetry Analysis grid, and mimics the Spectralis OCT printouts for within-eye Asymmetry Analysis. A color version of this figure is available online at www.optvissci.com.

Table 1

Means and standard deviations of retinal thicknesses (after we averaged superior and inferior retinal thicknesses) and within-eye asymmetry analyses for all five zones.

	Young group (21–35 years)		Older group (40–85 years)	
	Retinal Thickness	Asymmetry Analysis	Retinal Thickness	Asymmetry Analysis
Zones	Mean ± SD (μm)	Mean ± SD (μm)	Mean ± SD (μm)	Mean ± SD (μm)
1	331.34 ± 11.86	−1 ± 3.0	326.63 ± 11.64	−0.8 ± 2.6
2	333.04 ± 13.39	3.0 ± 5.3	320.65 ± 10.72	0.3 ± 5.8
3	297.09 ± 10.62	−2 ± 4.7	286.17 ± 10.50	−2.0 ± 5.0
4	278.83 ± 10.70	8.0 ± 6.1	268.71 ± 9.95	3.2 ± 6.7
5	301.58 ± 14.71	2.0 ± 10	293.12 ± 13.44	−1.6 ± 11.4
Whole Retinal Thickness	308.38 ± 11.21	−1 ± 3.0	299.06 ± 9.71	−0.8 ± 2.6

Optom Vis Sci. Author manuscript; available in PMC 2015 May 01.